

# Functional Association of the $\beta_1$ Subunit with Human Cardiac (hH1) and Rat Skeletal Muscle ( $\mu 1$ ) Sodium Channel $\alpha$ Subunits Expressed in *Xenopus* Oocytes

H. BRADLEY NUSS, NIPAVAN CHIAMVIMONVAT,  
M. TERESA PÉREZ-GARCÍA, GORDON F. TOMASELLI,  
and EDUARDO MARBÁN

From the Department of Medicine, The Johns Hopkins University, Baltimore, Maryland 21205

**ABSTRACT** Native cardiac and skeletal muscle Na channels are complexes of  $\alpha$  and  $\beta_1$  subunits. While structural correlates for activation, inactivation, and permeation have been identified in the  $\alpha$  subunit and the expression of  $\alpha$  alone produces functional channels,  $\beta_1$ -deficient rat skeletal muscle ( $\mu 1$ ) and brain Na channels expressed in *Xenopus* oocytes do not gate normally. In contrast, the requirement of a  $\beta_1$  subunit for normal function of Na channels cloned from rat heart or human heart (hH1) has been disputed. Coinjection of rat brain  $\beta_1$  subunit cRNA with hH1 (or  $\mu 1$ )  $\alpha$  subunit cRNA into oocytes increased peak Na currents recorded 2 d after injection by 240% (225%) without altering the voltage dependence of activation. In  $\mu 1$  channels, steady state inactivation was shifted to more negative potentials (by 6 mV,  $p < 0.01$ ), but the shift of 2 mV was not significant for hH1 channels. Nevertheless, coexpression with  $\beta_1$  subunit speeded the decay of macroscopic current of both isoforms. Ensemble average hH1 currents from cell-attached patches revealed that coexpression of  $\beta_1$  increases the rate of inactivation (quantified by time to 75% decay of current;  $p < 0.01$  at  $-30$ ,  $-40$ , and  $-50$  mV). Use-dependent decay of hH1 Na current during repeated pulsing to  $-20$  mV (1 s, 0.5 Hz) after a long rest was reduced to  $16 \pm 2\%$  of the first pulse current in oocytes coexpressing  $\alpha$  and  $\beta_1$  subunits compared to  $35 \pm 8\%$  use-dependent decay for oocytes expressing the  $\alpha$  subunit alone. Recovery from inactivation of  $\mu 1$  and hH1 Na currents after 1-s pulses to  $-20$  mV is multiexponential with three time constants; coexpression of  $\beta_1$  subunit decreased all three recovery time constants. We conclude that the  $\beta_1$  subunit importantly influences the function of Na channels produced by coexpression with either the hH1 or  $\mu 1$   $\alpha$  subunits.

Address correspondence to Eduardo Marbán, M.D., Ph.D., Division of Cardiology, 844 Ross Building, Johns Hopkins University, 720 North Rutland Avenue, Baltimore, MD 21205.

## INTRODUCTION

Sodium channels are pore-forming transmembrane proteins that selectively pass  $\text{Na}^+$  ions down their electrochemical gradient in response to membrane depolarization. An inward flow of  $\text{Na}^+$  ions generates the depolarizing current which initiates the rapid action potentials of nerve, skeletal muscle, and heart. Sodium channels in skeletal and ventricular muscle are complexes of a large  $\alpha$  subunit (260 kD) and a smaller noncovalently associated  $\beta_1$  subunit (38 kD for skeletal muscle, 36 kD for cardiac) (Sutkowski and Catterall, 1990; Isom, De Jongh, and Catterall, 1994). Mammalian brain Na channels are composed of three subunits; the additional  $\beta_2$  (33 kD) subunit is covalently linked by a disulfide bond to the  $\alpha$  subunit (Sutkowski and Catterall, 1990). The  $\alpha$  subunit contains at least 24 membrane-spanning segments, while the smaller  $\beta_1$  subunit has a lengthy extracellular domain, a short intracellular domain and a single membrane-spanning segment (Catterall, 1994).

The  $\alpha$  subunit encodes a transmembrane protein with the essential functions of an Na channel, including voltage-dependent gating and  $\text{Na}^+$  selectivity (Goldin, Snutch, Lubbert, Dowsett, Marshall, Auld, Downey, Fritz, Lester, Dunn, Catterall, and Davidson, 1986). However,  $\beta_1$ -deficient rat skeletal muscle and brain Na channels do not function normally (Krafte, Snutch, Leonard, Davidson, and Lester, 1988; Zhou, Potts, Trimmer, Agnew, and Sigworth, 1991; Cannon, McClatchey, and Gusella, 1993). The currents inactivate slowly compared to those recorded in native channels and the voltage dependence of inactivation is shifted to more positive potentials. Coinjection of rat brain and skeletal muscle  $\alpha$  subunit RNA with the rat or human brain  $\beta_1$  subunit RNA in *Xenopus* oocytes restores normal rapid inactivation, shifts the voltage dependence of inactivation to more negative potentials, increases the size of the current and relieves use-dependent decay (Auld, Goldin, Krafte, Marshall, Dunn, Catterall, Lester, Davidson, and Dunn, 1988; Isom, DeJongh, Patton, Reber, Offord, Charbonneau, Walsh, Goldin and Catterall, 1992; Cannon et al., 1993).

Despite biochemical evidence for a functional association of  $\alpha$  and  $\beta_1$  subunits in heart muscle and the abundant expression of  $\beta_1$  subunits in heart as well as in skeletal muscle and brain (Sutkowski and Catterall, 1990; Makita, Bennett, and George, 1994; Wallner, Weigl, Meera, and Lotan, 1993), the requirement of  $\beta_1$  for normal function of cardiac Na channels expressed in oocytes has been disputed. Cardiac Na channels expressed in oocytes from a subunit RNA have been reported to possess normal physiologic properties (Krafte, Volberg, Dillon, and Ezrin, 1991) and macroscopic current kinetics characteristic of native cardiac Na channels (Gellens, George, Chen, Chahine, Horn, Barchi, and Kallen, 1992; Satin, Kyle, Chen, Rogart, and Fozzard, 1992). In contrast to findings in skeletal muscle Na channels, it has been reported that the human  $\beta_1$  subunit ( $\text{H}\beta_{1A}$ ) does not functionally modify the human heart Na channel when both the hH1  $\alpha$  and  $\text{H}\beta_{1A}$  subunits are coinjected into *Xenopus* oocytes (Makita et al., 1994). Our observations indicate that co-expression of  $\beta_1$  with the hH1  $\alpha$  subunit in oocytes has several effects. First, co-expression dramatically increases the current density; second, inactivation is accelerated; and finally, use-dependent decay of the Na current is markedly reduced and recovery from inactivation is accelerated. Our data support an impor-

tant functional association between the  $\beta_1$  subunit and both the hH1 and  $\mu 1$   $\alpha$  subunits.

## MATERIALS AND METHODS

### *Preparation of cRNA*

In vitro transcription of complementary RNA (cRNA) for injection into oocytes was initiated by restriction enzyme digestion of the full-length cDNA constructs subcloned into the pSP64T\* vector (Krieg and Melton, 1984). Plasmid DNA was linearized by digestion with XbaI (hH1), Sall ( $\mu 1$ ), or EcoRI ( $\beta_1$ ) which recognized sites beyond the 3' noncoding region of the insert DNA. After phenol/chloroform (1:1) and chloroform/isoamyl alcohol (24:1) extractions, the linearized DNA was precipitated (3 M NaOAc, pH 5.2), washed with ethanol (70%) and vacuum dried. The in vitro transcription reactions were carried out by the addition of 2  $\mu$ l SP6 RNA polymerase (GIBCO BRL, Gaithersburg, MD) to a buffer solution comprised of transcriptional buffer (20  $\mu$ l), dithiothreitol (10  $\mu$ l, 0.1 M), RNase inhibitor (2.5  $\mu$ l), ribonucleotide triphosphates (10  $\mu$ l of 10 $\times$  stock, Promega Corp., Madison, WI), diguanosine triphosphate (10  $\mu$ l), diethyl pyrocarbonate-deionized H<sub>2</sub>O (35.5  $\mu$ l), and DNA (10  $\mu$ l) at 37°C for 6 h. Additional RNA polymerase (2  $\mu$ l) was added after the first 3 h. After a short incubation (15 min, 37°C) with RQ1 DNase (4  $\mu$ l; Promega Corp.), addition of 5  $\mu$ l EDTA (0.5 M, pH 8.0) stopped the reaction. After extraction, precipitation and ethanol wash, the integrity of the RNA was verified by electrophoresis on an agarose gel (1%). The final concentration of hH1 and  $\mu 1$   $\alpha$  subunit mRNA was adjusted to 1  $\mu$ g/ $\mu$ l, while  $\beta_1$  subunit RNA was left undiluted at concentrations ranging from 5–6  $\mu$ g/ $\mu$ l. The clones for hH1 (Gellens et al., 1992),  $\mu 1$  (Trimmer, Cooperman, Tomiko, Zhou, Crean, Boyle, Kallen, Sheng, Barchi, Sigworth, Goodman, Agnew, and Mandel, 1989) and rat brain  $\beta_1$  (Isom et al., 1992) were provided by R. G. Kallen (University of Pennsylvania, Philadelphia, PA), Gail Mandel (State University of New York at Stony Brook, Stony Brook, NY) and W. A. Catterall (University of Washington, Seattle, WA), respectively. A large portion of the 3' untranslated region of the hH1 cDNA vector was eliminated using PCR mutagenesis because it contained ambiguous sequence.

### *Expression in Xenopus laevis Oocytes*

Adult female *Xenopus laevis* (Xenopus 1; Ann Arbor, MI or Nasco, Ft. Atkinson, WI) were anesthetized with 3-aminobenzoic acid ethyl ester (methanesulfonate salt, 0.17%, Sigma Chemical Co., St. Louis, MO). Sections of ovarian lobes were surgically removed through a small incision in the abdomen and placed in sterile ND-96 solution (96 mM NaCl, 2 mM KCl, 1 mM MgCl<sub>2</sub>, 1.8 mM CaCl<sub>2</sub>, 5 mM HEPES, pH 7.6, with NaOH). The ovarian lobes were teased into small clumps of oocytes, placed into centrifuge tubes and rinsed in Ca<sup>2+</sup>-free OR-2 solution (82.5 mM NaCl, 2.5 mM KCl, 1 mM MgCl<sub>2</sub>, 5 mM HEPES, pH 7.6, with NaOH). Two periods (30–45 min) of collagenase (1–2 mg/ml in Ca<sup>2+</sup>-free OR-2, Type 1A; Sigma Chemical Co., St. Louis, MO) digestion with mild agitation on an orbital shaker freed individual oocytes from the ovarian lobes and removed the surrounding follicular cell layer. After digestion, stage V and VI oocytes were placed in ND-96 supplemented with penicillin (100 U/ml), streptomycin (100  $\mu$ g/ml), sodium pyruvate (2 mM), and theophylline (0.5 mM).

Oocytes with a distinct equatorial band between the animal and vegetal poles were injected with 50–100 nl of mRNA using a 10- $\mu$ l microinjector (Drummond Scientific Co., Broomall, PA) to express  $\mu 1$  and hH1 channels. Oocytes were coinjected with 50–100 nl of mRNA solution containing a 1:1 volume ratio of  $\alpha$  to  $\beta_1$  subunit mRNA to express  $\mu 1$ - $\beta_1$  or hH1- $\beta_1$  channels. Since the  $\beta_1$  subunit mRNA was more concentrated than the  $\alpha$  subunit mRNA,  $\beta_1$  was coinjected in five- to sixfold excess of the  $\alpha$  subunit. Using this procedure we estimate that the amount of injected  $\beta_1$  mRNA sufficed to enable the majority of the expressed  $\alpha$  subunits to associate with a  $\beta_1$  subunit (Cannon

et al., 1993). Injected oocytes were incubated for 1–5 d at room temperature until the desired expression level was achieved.

#### *Two-Electrode Recording of Macroscopic $I_{Na}$*

Macroscopic  $\mu$ l and hH1 Na currents were recorded using a two-microelectrode voltage clamp technique (Methfessel, Witzemann, Takahashi, Mishina, Numa, and Sakmann, 1986). The whole-cell recording solution was ND-96. Both voltage and current electrodes were pulled from 1.2-mm OD borosilicate glass (World Precision Instruments Inc., Sarasota, FL) on a two-stage vertical puller (Narishige Tokyo, Japan). When filled with 3 M KCl, the electrodes had resistances of 0.2–0.4 M $\Omega$ . Membrane potential was controlled by a two-electrode voltage clamp amplifier with a virtual ground circuit (Warner Instruments Corp., Hamden, CT). Current signals were low-pass filtered at 1 kHz by an 8-pole Bessel filter (Frequency Devices Inc., Haverhill, MA) and digitized on-line at 10–20 kHz with 12-bit resolution onto a personal computer. All electrophysiological recordings were obtained at room temperature (20–22°C).

Oocytes accepted for study had stable membrane potentials more negative than –25 mV and holding currents that remained < –0.01  $\mu$ A at –100 mV for the duration of the experiment. During two-electrode voltage clamp recording, precautions were taken to avoid voltage escape or a loss of voltage control. Experiments with over-compensation artifacts evident as notches in the current elicited by steps to positive potentials or in the tail currents evoked upon repolarization were not analyzed. Likewise, experiments with artifacts such as an “abominable notch” (Cole, 1972) were also excluded from study. When determining the whole-cell current-voltage relationships, all experiments included in the analysis had currents that activated in a graded fashion during progressive 5-mV depolarizing steps. When determining the voltage dependence of steady state inactivation, the only experiments analyzed were those in which the times to peak current measured with all ( $h_{\infty} = 1$ ) and half ( $h_{\infty} = 0.5$ ) the channels available differed by <10%.

#### *Single-Channel Current Recordings*

Oocytes were first screened to determine the level of Na channel expression: those expressing macroscopic currents in excess of 4  $\mu$ A were selected for patch clamp experiments. After screening, the vitelline membrane was microdissected away during incubation of the oocytes in a hyperosmolar solution (462 mOsm) comprised of 220 mM *N*-methyl-D-glucamine (NMG), 220 mM aspartic acid, 2 mM MgCl<sub>2</sub>, 10 mM EGTA, 10 mM HEPES, pH 7.2, with NMG.

Depolarizing high-potassium bath solution containing 140 mM KCl, 10 mM HEPES, pH 7.4, was used to zero the membrane potential. Pipettes were filled with recording solution consisting of 140 mM NaCl, 1 mM BaCl<sub>2</sub>, 10 mM HEPES, 7.4 pH. Patch pipettes, fabricated from borosilicate glass, coated near the tip with Sylgard (Dow Corning, Midland, MI) and fire polished to adjust tip diameter, had resistances of 10–15 M $\Omega$  when filled with recording solution. An Axopatch 200 amplifier with CV-202 headstage (Axon Instruments, Foster City, CA) was used to record currents in the cell-attached configuration. Voltage pulse protocols, data acquisition and analysis were performed by custom-written software and executed on a personal computer. Current recordings were filtered at 2 or 5 kHz when sampling every 100 or 50  $\mu$ s, respectively, and digitized on-line at 10–20 kHz with 12-bit resolution.

Capacity transients and passive leak currents were subtracted using a curve-fitted blank sweep as a leak template. Only fully resolved single-level openings were used to construct amplitude distributions. Amplitude histograms were fit by Gaussian functions (Origin, MicroCal Software Inc., Northampton, MA) to determine the unitary current amplitude at each test potential. Ensemble average currents were constructed from patches containing four or more and often in excess of 10 active channels as judged from the number of stacked openings. These data were collected by repeatedly cycling through a family of potentials from –60 to –20 mV using a 2-s repetition interval

and recording from each patch for at least 25 min. These records were idealized using a half-height criterion (Colquhoun and Sigworth, 1983) with three-point detection. The ensemble averages of the idealized currents at each potential were used for kinetic analysis.

#### *Curve Fitting Functions*

The macroscopic current-voltage relationships were fit with a combined Boltzmann and Goldman-Hodgkin-Katz equation (Hille, 1992) to determine half-activation potentials. Voltage dependence of inactivation relationships ( $h_\infty$  curves) were fit with a standard Boltzmann equation. The recovery from inactivation data were fit by exponential decay functions. A Gaussian function was used to fit the single-channel current amplitude histograms.

#### *Statistical Analysis*

All data are presented as means and standard errors. Significance of differences between two populations ( $\alpha$  vs  $\alpha\text{-}\beta_1$ ) over a range of voltages was assessed using multivariate analysis of variance (MANOVA, Systat Inc., Evanston, IL). Data at individual voltages were compared by unpaired two-sided  $t$  tests. Differences were considered statistically significant when  $p < 0.02$ .

### RESULTS

#### *Coinjection of the $\beta_1$ Subunit Increases Functional Na Channel Expression*

Sodium currents recorded in oocytes injected with RNA encoding the  $\mu 1$  skeletal muscle Na channel  $\alpha$  subunit were compared to  $I_{Na}$  recorded in oocytes coinjected with excess  $\beta_1$  subunit. With the holding potential set at  $-100$  mV, step depolarizations to voltages from  $-60$  to  $30$  mV evoked families of currents shown in Fig. 1. The rate of macroscopic current decay is dramatically increased by coexpression with the  $\beta_1$  subunit (Fig. 1 A). The similarity of the descending limbs of the peak current-voltage relationships (Fig. 1 B) suggests that the voltage dependence of activation in  $\mu 1$  channels is not significantly influenced by the  $\beta_1$  subunit. Indeed, the half-activation potentials equal  $-27 \pm 1$  mV for  $\mu 1$  ( $n = 10$  and  $13$ ) and  $-26 \pm 1$  mV for  $\mu 1\text{-}\beta_1$  ( $n = 4$  and  $6$ ). The ascending limbs of the current-voltage relationships are significantly different ( $p < 0.001$ ), possibly due to rapid inactivation of  $\mu 1\text{-}\beta_1$  currents at positive potentials. Coexpression with  $\beta_1$  subunit increased the expression of peak  $I_{Na}$  measured one day after injection to  $-6.2 \pm 0.9$   $\mu\text{A}$  ( $n = 27$ ) from  $-1.9 \pm 0.2$   $\mu\text{A}$  in  $\mu 1$  Na channels alone ( $n = 14$ ,  $p < 0.001$ , Fig. 1 B, *inset*). Na currents recorded two days after injection of the  $\alpha$  subunit alone ( $-6.0 \pm 0.7$   $\mu\text{A}$ ,  $n = 40$ ) equaled the level of expression that the coinjected ( $\mu 1\text{-}\beta_1$ ) oocytes had achieved in just one day and did not significantly increase further by day 3.

While the inactivation kinetics of the whole-cell Na currents recorded in oocytes injected with the hH1  $\alpha$  subunit RNA are intrinsically faster than those of  $\mu 1$  Na currents, coexpression with the  $\beta_1$  subunit further hastens the decay of hH1 Na currents during maintained depolarization (Fig. 2 A). (This kinetic effect is analyzed in detail below, based on patch recordings.) As was the case with  $\mu 1$ , coinjection of  $\beta_1$  increased the hH1 peak current density (Fig. 2 B, *inset*). Families of Na currents were recorded in oocytes injected with either the hH1  $\alpha$  subunit alone or in tandem with the  $\beta_1$  subunit at days 1, 2, 3, and 4 (hH1 only) after injection. Coinjection with the  $\beta_1$  subunit increased the size of  $I_{Na}$  over the entire range of po-

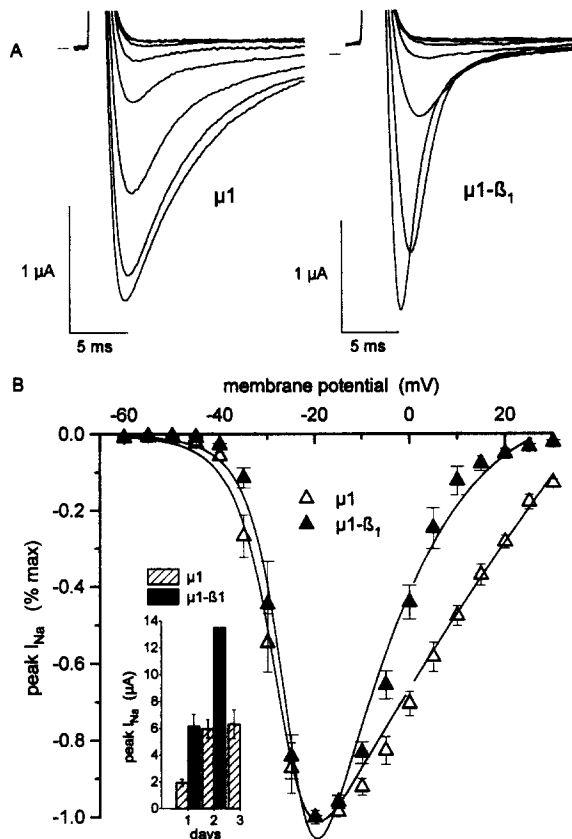


FIGURE 1. Macroscopic  $\mu 1$  and  $\mu 1-\beta_1$  currents (A), normalized current-voltage relationships (B) and comparison of expression levels of  $\mu 1$  and  $\mu 1-\beta_1$  Na channels (B, inset). Families of currents were elicited from  $-100$  mV by progressive step depolarizations (40 ms) starting at  $-60$  mV and ending at  $+30$  mV. The currents shown were recorded at  $-60$ ,  $-50$ ,  $-45$ ,  $-40$ ,  $-35$ ,  $-30$ ,  $-25$ , and  $-20$  mV. Measurements of peak current were made with respect to the baseline current at 40 ms and normalized to the largest peak current recorded. The mean data were fit to combined Boltzmann and Goldman-Hodgkin-Katz equations. The half-activation potentials equaled  $-27 \pm 1$  mV for  $\mu 1$  ( $n = 10$  and 13, open triangles) and  $-26 \pm 1$  mV for  $\mu 1-\beta_1$  ( $n = 4$  and 6, solid triangles). The bar graph (B, inset) illustrates that the level of  $\mu 1$  current expressed increases more than twofold by coinjection of the  $\beta_1$  subunit (see Results for details).

tentials ( $-55$  mV to  $+20$  mV, not shown). Peak  $I_{Na}$  measured in hH1- $\beta_1$  oocytes was always larger than that recorded in oocytes injected with the  $\alpha$  subunit alone ( $p < 0.001$ ). When the means of the normalized current-voltage relationships were fit using combined Boltzmann and Goldman-Hodgkin-Katz equations (Fig. 2 B), there was no significant difference in the half-activation potentials for hH1 ( $V_{1/2} = -6 \pm 1$  mV,  $n = 30$ ) and hH1- $\beta_1$  ( $V_{1/2} = -37 \pm 1$  mV,  $n = 8$  and 14) channels.

#### Permeation Is Not Altered by $\beta_1$ Association

We used single-channel recordings to try to understand the mechanism of the changes in the macroscopic currents. Measurements from cell-attached patches indicate that unitary current amplitudes ( $i$ ) are not altered by coexpression of the  $\beta_1$  subunit with  $\mu 1$  and hH1  $\alpha$  subunits. Amplitude histograms were constructed from clearly resolved openings to determine  $i$  for  $\mu 1$  (Fig. 3) and hH1 (Fig. 4) channels at potentials between  $-70$  and  $-10$  mV. At any given potential, unitary current amplitudes of channels expressed from  $\alpha$  only or from  $\alpha-\beta_1$  were indistinguishable. The slope conductance measured  $32.3 \pm 0.1$  pS for  $\mu 1$   $\alpha$ -only channels ( $n = 32$ ) and  $29.5 \pm 0.2$  pS for hH1  $\alpha$ -only channels ( $n = 25$ ); neither was significantly al-

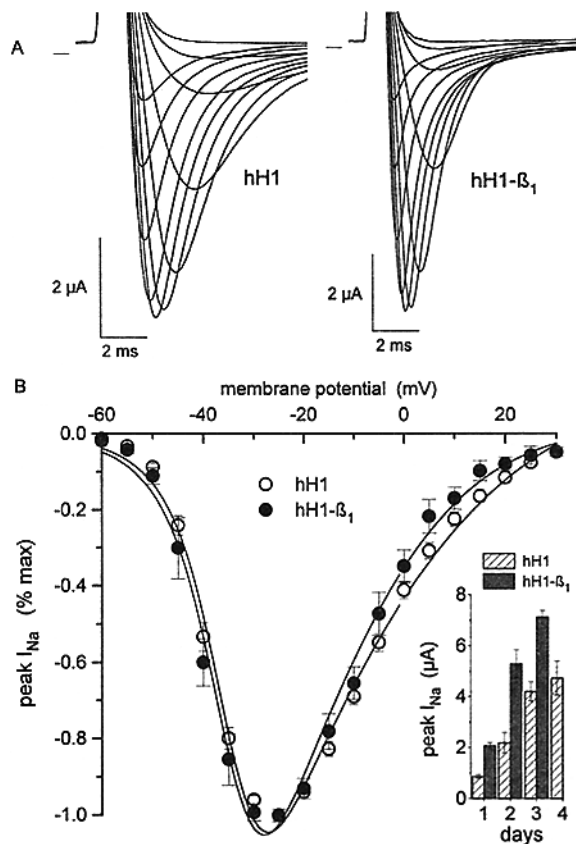


FIGURE 2. Macroscopic hH1 and hH1- $\beta_1$  currents (A), normalized current-voltage relationships (B) and comparison of expression of hH1 hH1- $\beta_1$  Na channels (B, inset). Families of currents were elicited from -100 mV by progressive step depolarizations (20 ms) starting at -60 mV and ending at +30 mV. Comparison of similarly sized currents (A) recorded at -60, -50, -45, -40, -35, -30, -25, -20, -10, 0, and +10 mV and shown at the same time base demonstrates that coexpressed channels have hastened inactivation kinetics. Normalized current-voltage relationships (B) for hH1 and hH1- $\beta_1$  macroscopic currents show no significant difference in the half-activation potentials for hH1 ( $-36 \pm 1$  mV,  $n = 30$ , open circles) and hH1- $\beta_1$  ( $-37 \pm 1$  mV,  $n = 8$  and 14, solid circles) currents. The mean data were fit to combined Boltzmann and Goldman-Hodgkin-Katz equations to determine the half-activation potentials. A bar graph (B,

inset) summarizes measurements of peak  $I_{Na}$  at successive days after injection of RNA into oocytes. The level of hH1 current expressed at days 1, 2, and 3 (day 1 =  $-0.9 \pm 0.1$   $\mu A$ ,  $n = 9$ ; day 2 =  $-2.2 \pm 0.4$   $\mu A$ ,  $n = 24$ ; day 3 =  $-4.2 \pm 0.4$   $\mu A$ ,  $n = 14$ ) was significantly ( $p < 0.001$ ) increased by coinjection with the  $\beta_1$  subunit (day 1 =  $-2.1 \pm 0.1$   $\mu A$ ,  $n = 31$ ; day 2 =  $-5.3 \pm 0.6$   $\mu A$ ,  $n = 17$ ; day 3 =  $-7.1 \pm 0.3$   $\mu A$ ,  $n = 9$ ) ( $p < 0.001$ ).

tered by coexpression with the  $\beta_1$  subunit ( $32.3 \pm 0.2$  pS for  $\alpha 1$ - $\beta_1$ ,  $n = 29$  and  $29.0 \pm 0.2$  pS for hH1- $\beta_1$  channels,  $n = 26$ ). The lack of any changes in the open-channel properties indicates that the increase in whole-cell current reflects an increase in functional channels and/or changes in unitary gating, as considered further in the Discussion.

*The Voltage Dependence of Inactivation Is Left-shifted in Oocytes Coinjected with the  $\beta_1$  Subunit*

Coexpression of rat brain IIA and skeletal muscle Na channels with the  $\beta_1$  subunit has been shown to shift the voltage dependence of inactivation to more negative potentials, closer to the gating behavior found in native channels (Isom et al., 1992; Cannon et al., 1993). We confirmed these results in  $\mu 1$ -injected oocytes (Fig. 5)

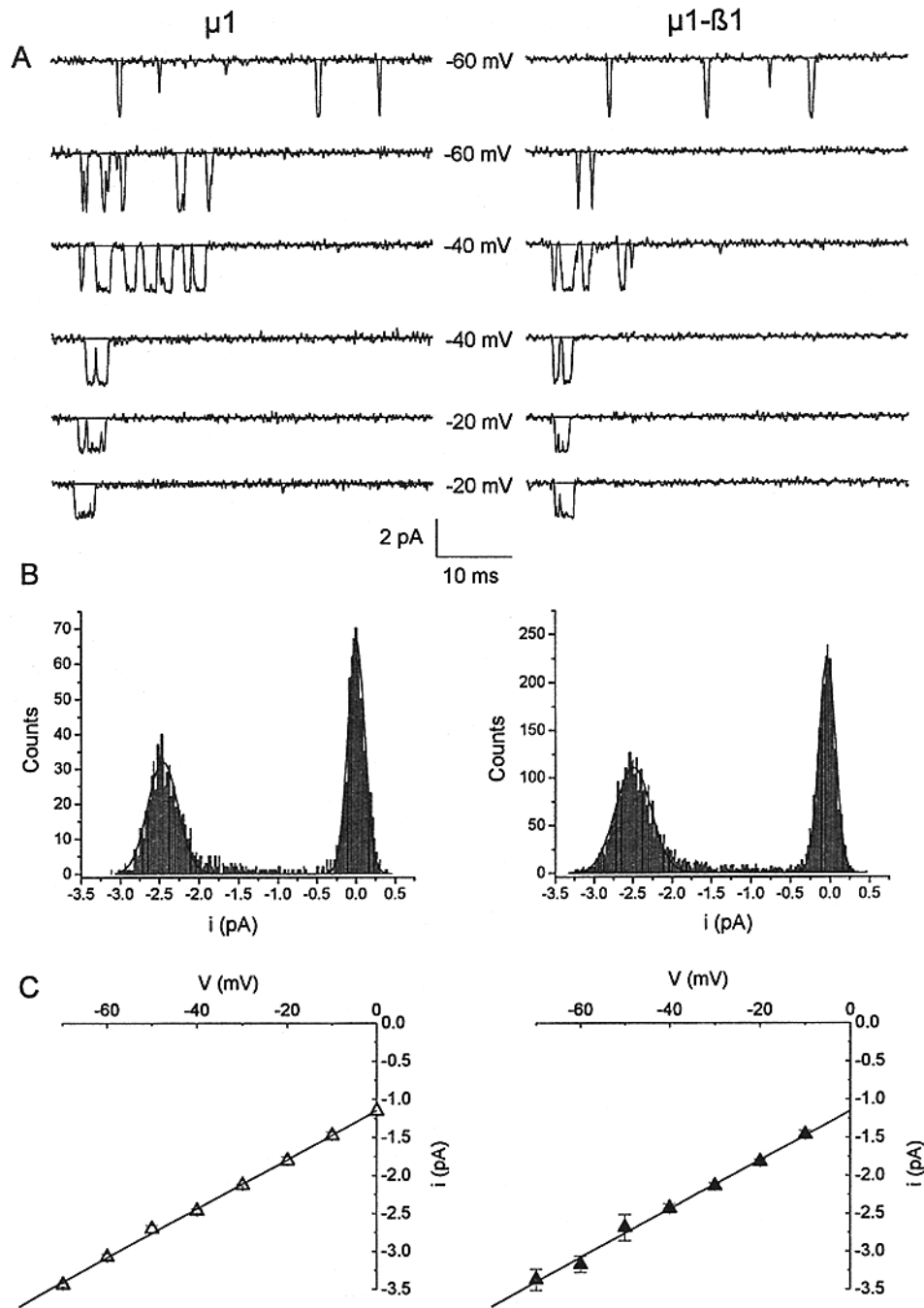


FIGURE 3. Single-channel currents (A), amplitude histograms (B) and unitary current-voltage relationships (C) for  $\mu 1$  and  $\mu 1-\beta 1$  Na channels. Single-channel current amplitude ( $i$ ) determined by amplitude histograms (B) equaled  $-2.46 \pm 0.03$  pA for  $\mu 1$  ( $n = 8$ ) and  $-2.43 \pm 0.06$  pA for  $\mu 1-\beta 1$  channels ( $n = 6$ ) at  $-40$  mV. The unitary current-voltage relationships (C) were not altered: slope conductance equaled  $32.3 \pm 0.1$  pS in  $\mu 1$  channels ( $n = 32$ ) and  $32.3 \pm 0.3$  pS in  $\mu 1-\beta 1$  channels ( $n = 29$ ).



and tested for a similar  $\beta_1$  effect on the voltage dependence of inactivation in hH1-injected oocytes (Fig. 6). Peak  $I_{Na}$  availability was measured by a test depolarization to  $-20$  mV after a 1-s conditioning prepulse. The prepulse potential was varied from  $-140$  mV to progressively more depolarized potentials to inactivate greater numbers of channels. A repetition interval of 15 s allowed for full recovery of  $I_{Na}$  from the inactivation which occurs during a 1-s prepulse. Coinjection of  $\beta_1$  resulted in a 6-mV hyperpolarizing shift in the half-inactivation voltages to  $-60 \pm 1$  mV ( $n = 6$ ) from  $-54 \pm 1$  mV ( $n = 8$ ) in  $\mu 1$ -injected oocytes ( $p < 0.001$ ). The raw current tracings shown in Fig. 5 A illustrate a greater fraction of Na channels inactivated by a prepulse to  $-60$  mV in  $\mu 1$ - $\beta_1$  than in  $\mu 1$  oocytes.

For hH1, representative records illustrate that slightly more hH1- $\beta_1$  current is inactivated by a prepulse to  $-75$  mV than in an hH1-alone oocyte (Fig. 6 A). Pooled data reveal that the voltage dependence of inactivation in oocytes expressing hH1 Na channels was shifted to more negative potentials by coinjection with the  $\beta_1$  subunit (Fig. 6), albeit to a lesser extent than was the case for  $\mu 1$ . The half-inactivation potential was changed by only 2 mV, to  $-78 \pm 1$  mV in hH1- $\beta_1$  oocytes ( $n = 9$ ) from  $-76 \pm 1$  mV in hH1 oocytes ( $n = 9$ ,  $p = \text{NS}$ ).

#### *Coexpression of the $\beta_1$ Subunit Speeds Activation and Inactivation*

The decay of macroscopic  $\mu 1$  current during maintained depolarization was increased in oocytes coexpressing  $\alpha$  and  $\beta_1$  subunits (Figs. 1 and 5). Coexpression of the  $\beta_1$  subunit also speeds up the decay of macroscopic hH1 Na currents, albeit to a lesser extent than for  $\mu 1$  Na currents (Figs. 2 and 6). Recordings from cell-attached patches containing  $\mu 1$ ,  $\mu 1$ - $\beta_1$ , hH1, and hH1- $\beta_1$  Na channels verified that the observed differences in the inactivation kinetics of the macroscopic currents recorded using two-electrode voltage clamp were genuine. The ensemble average currents shown in Fig. 7 were normalized and superimposed to facilitate the comparison of inactivation kinetics. The increased rate of inactivation of ensemble average currents (Fig. 7 A, shown at  $-40$  mV) recorded from oocytes coexpressing  $\alpha$  and  $\beta_1$  subunits is dramatic for  $\mu 1$  Na channels over a wide range of voltages ( $-60$  to  $0$  mV, data not shown). Similarly, in Fig. 7 B the ensemble averages (shown at  $-30$ ,  $-40$ , and  $-50$  mV) of coexpressed hH1- $\beta_1$  channels clearly inactivate more rapidly than ensembles constructed from  $\alpha$ -only channels (hH1).

The rates of inactivation of hH1- $\beta_1$  and hH1 channels were compared by measuring the times to 75% decay of ensemble average currents (Fig. 8 A,  $T_{75}$ ) at potentials between  $-60$  and  $-30$  mV. We chose to quantify  $T_{75}$  because it is a simple model-independent measure that does not require the assumption of single- or multi-exponential current decay. Voltage-dependent inactivation of hH1 and hH1- $\beta_1$  channels is evident in the superimposed ensemble averaged current records (Fig. 7 B) and in the  $T_{75}$  plot (Fig. 8 A). While hH1 currents decay faster than  $\mu 1$  currents, coexpression with the  $\beta_1$  subunit nevertheless significantly speeds the rate of inactivation of hH1- $\beta_1$  ensemble average currents at  $-50$ ,  $-40$ , and  $-30$  mV ( $p = 0.01$ ,  $0.01$ , and  $0.004$ , respectively, by unpaired two-sided  $t$  test). For example, at  $-40$  mV hH1- $\beta_1$  ensemble averaged currents decayed to 25% of their peak amplitude in  $1.5 \pm 0.3$  ms ( $n = 5$ ) as compared to  $2.8 \pm 0.3$  ms ( $n = 6$ ) for hH1. These data confirm that the  $\beta_1$ -induced hastening of inactivation of hH1 Na channels underlies the ac-

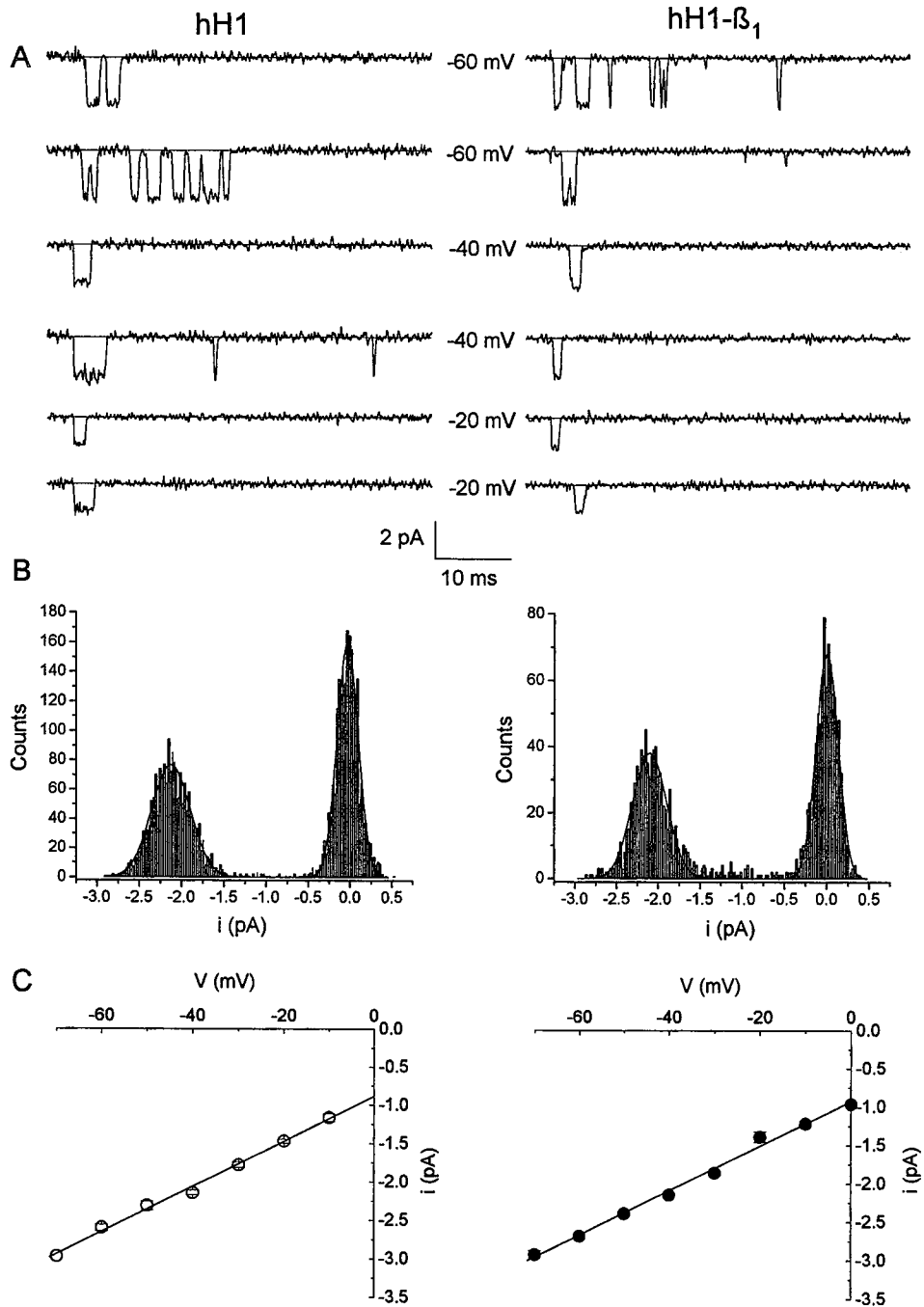


FIGURE 4. Single-channel currents (*A*), amplitude histograms (*B*) and unitary current-voltage relationships (*C*) for hH1 and hH1- $\beta_1$  Na channels. Single-channel current amplitude ( $i$ ) determined by amplitude histograms (*B*) equaled  $-2.14 \pm 0.03$  pA for hH1 ( $n = 6$ ) and  $-2.14 \pm 0.02$  pA for hH1- $\beta_1$  channels ( $n = 6$ ) at  $-40$  mV. The unitary current-voltage relationships (*C*) were not altered: slope conductance equaled  $29.5 \pm 0.2$  pS in hH1 channels ( $n = 25$ ) and  $29.0 \pm 0.2$  pS in hH1- $\beta_1$  channels ( $n = 26$ ).

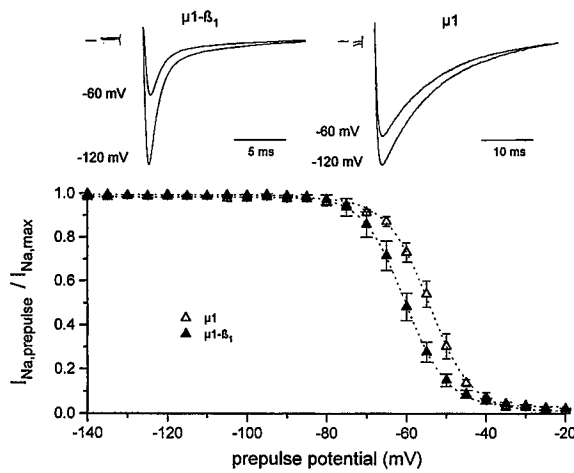


FIGURE 5. Voltage dependence of inactivation of  $\mu 1$  and  $\mu 1$ - $\beta_1$  Na channels. Measurements of peak currents elicited at  $-20$  mV immediately after a 1-s prepulse ( $-140$  to  $-20$  mV) define the relationship (B). Raw currents (shown with capacity transients blanked) in the upper panels (A) were recorded after prepulses to  $-120$  and  $-60$  mV. When the mean data were fit by a Boltzmann function, the half-inactivation potentials equaled  $-60 \pm 1$  mV for  $\mu 1$ - $\beta_1$  ( $n = 6$ , solid triangles) and  $-54 \pm 1$  mV for  $\mu 1$  ( $n = 8$ , open triangles).

celerated decay of the macroscopic Na current observed in whole-cell recordings with two-electrode voltage clamp (Figs. 2 and 6).

The results in Fig. 7 B further suggest that the activation of hH1 may be accelerated by coexpression with  $\beta_1$ . Although the pooled data for the times to peak of the ensemble average currents (Fig. 8 B) did confirm a tendency for hH1- $\beta_1$  channels to activate faster than hH1 channels, the differences did not reach statistical significance ( $p = 0.06$  by unpaired two-sided  $t$  test at  $-40$  mV).

*Relief of Use-dependent Decay of Peak Current by  $\beta_1$  Subunit*

Differences in the reduction of the peak current with repetitive pulsing provide strong evidence for a functional association between  $\alpha$  and  $\beta_1$  subunits in oocytes.

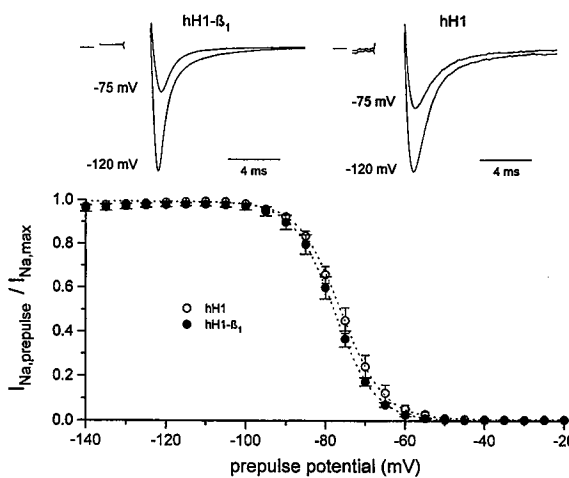


FIGURE 6. Voltage dependence of inactivation of hH1 and hH1- $\beta_1$  Na channels. Measurements of peak currents at  $-20$  mV immediately after a 1-s prepulse ( $-140$  to  $-20$  mV) define the relationships. Raw currents (shown with the capacity transients blanked) in the upper panels were recorded after prepulses to  $-120$  and  $-75$  mV. When the mean data (B) were fit by a Boltzmann function, the half-inactivation potentials equaled  $-78 \pm 1$  mV for hH1- $\beta_1$  ( $n = 9$ , solid circles) and  $-76 \pm 1$  mV for hH1 ( $n = 9$ , open circles).

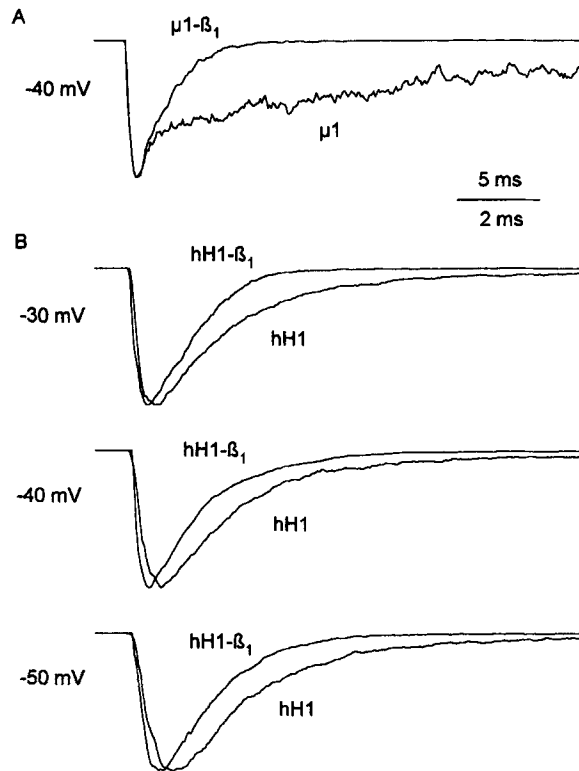


FIGURE 7. Ensemble average currents of  $\mu 1$  and  $\mu 1-\beta_1$  (A) and hH1 and hH1- $\beta_1$  (B) Na channels. Ensemble average currents were constructed from macro-patch recordings from cell-attached patches during repeated families of depolarizations ( $-60$  to  $-30$  mV, 0.5 Hz) while holding at  $-140$  mV between voltage steps. Ensemble average currents for  $\alpha$ -only and  $\alpha-\beta_1$  channels are superimposed and normalized to peak current. Peak  $\mu 1$  and  $\mu 1-\beta_1$  ensemble averages (A) shown at  $-40$  mV measured  $-1.2$  and  $-2.0$  pA, respectively. Peak hH1 and hH1- $\beta_1$  ensemble averages (B) shown at  $-30$ ,  $-40$ , and  $-50$  mV for the same two patches, measured  $-8$  to  $-11$  pA for the patch containing hH1 channels and  $-11$  to  $-17$  pA for the patch containing hH1- $\beta_1$  channels.

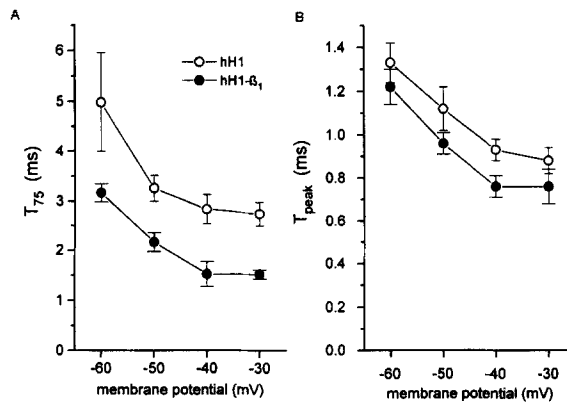


FIGURE 8. Analysis of inactivation (A) and activation (B) kinetics of ensemble average hH1 vs hH1- $\beta_1$  currents. Measurements of the time to 75% decay of current (A,  $T_{75}$ ) and time to peak current (B,  $T_{peak}$ ) were made from ensemble averages obtained at potentials between  $-60$  and  $-30$  mV of hH1- $\beta_1$  channels (solid circles) compared to hH1 (open circles) channels. The decrease in  $T_{75}$  was significant at  $-50$ ,  $-40$ , and  $-30$  mV ( $p = 0.01$ ,  $0.01$ , and  $0.004$ , respectively).

tively,  $n = 6$ ); the  $\beta_1$ -induced reduction in  $T_{75}$  measured at  $-60$  mV did not reach significance because of the large variability in the decay phase of the hH1 ensemble averages, which were the smaller and noisier at  $-60$  mV compared to hH1- $\beta_1$ . The reduction in  $T_{peak}$  did not reach statistical significance at any potential studied ( $p = 0.06$  at  $-40$  mV,  $n = 6$ ).

Currents were elicited by trains of short (Fig. 9 A, 10 ms) and long (Fig. 9 B, 1 s) voltage steps to  $-20$  mV after a long rest ( $>45$  s) at a repetition interval of 2 s. Peak  $I_{Na}$  was measured for each of the first 20 pulses in the train. This protocol provides an indirect measure of the accumulation of channels in the inactivated state. The extent of use dependence is a function of a particular channel type and its ability to recover from fast and slow inactivation. Let us first consider the  $\mu 1$  channel. In the absence of the  $\beta_1$  subunit, a substantial reduction in the peak current is already evident by the second voltage pulse in the train (Fig. 9). Second pulse  $\mu 1$  currents equaled  $91 \pm 2\%$  and  $55 \pm 1\%$  of the first short and long pulses, respectively. With continued pulsing, the decay became even more pronounced, so that at pulse 20 the percentage of  $\mu 1$  current remaining measured  $84 \pm 3\%$  and  $46 \pm 5\%$  of the first pulse current for short and long pulse durations, respectively. The comparable steady state values for oocytes coexpressing the  $\beta_1$  subunit equaled  $98 \pm 1\%$  and  $83 \pm 2\%$  of the first pulse current. Thus, the presence of the  $\beta_1$  subunit significantly reduced the use-dependent decay of the peak  $\mu 1$  current by both short and long duration pulse trains ( $p < 0.001$ ,  $n = 6$ ).

The same experimental protocol was used to compare the use-dependent properties of hH1 and hH1- $\beta_1$  channels (Fig. 9). In contrast to the results with  $\mu 1$ , trains

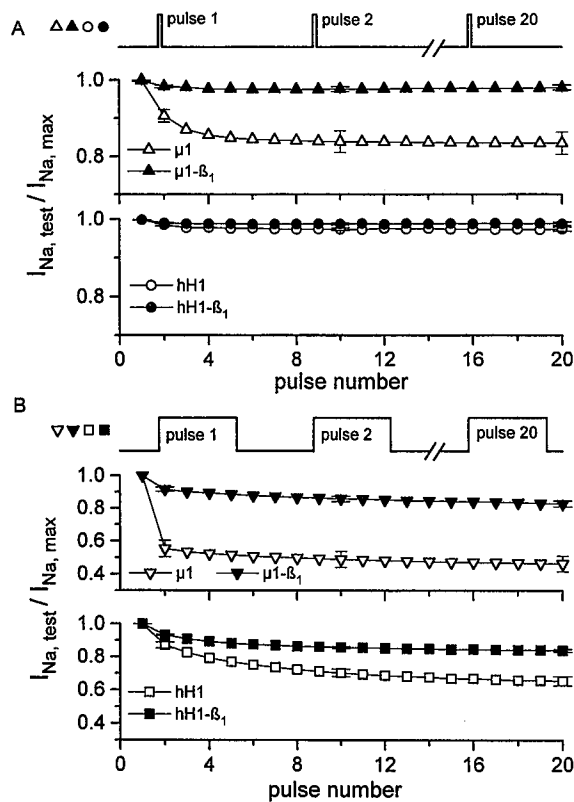


FIGURE 9. Use-dependent decay of peak  $\mu 1$  and hH1 Na currents is reduced by coinjection with  $\beta_1$ . Step depolarizations at 0.5 Hz of 10 ms (A) or 1 s (B) were initiated after a long rest as illustrated by the voltage pulses shown above the plots. Measurements of peak currents were normalized to the first pulse current and plotted as a function of pulse number. Decay of  $\mu 1$  current (open triangles) is pronounced even with 10-ms pulses (A). Coexpression of the  $\beta_1$  subunit dramatically reduces use-dependent decay of  $\mu 1$ - $\beta_1$  current (solid triangles). Although the decay of hH1 current which occurs during a train of short pulses is small (3%), decay of hH1 current with 1 s pulses (B, open squares) is pronounced. Coexpression of the  $\beta_1$  subunit dramatically reduces use-dependent decay current during the 1-s pulse train (B, solid squares, see Results for details).

of short pulses (Fig. 9, *upper panels*) resulted in a very small decrement of hH1 current ( $97 \pm 1\%$ ,  $n = 10$ ). The inclusion of the  $\beta_1$  subunit produced a small but significant amount of relief of the use-dependent decay of peak hH1- $\beta_1$  current ( $99 \pm 1\%$ ,  $n = 10$ ,  $p < 0.001$ ). The  $\beta_1$ -induced reduction in use dependence was more apparent when trains of long-duration pulses (Fig. 9 *B*) were used. Pulse 2 hH1 current was reduced to  $87 \pm 2\%$  ( $n = 10$ ) of the first pulse current. Use-dependent decay of hH1 current developed progressively during the remainder of the pulse train such that, by pulse 20, peak hH1 current was reduced to  $65 \pm 3\%$  ( $n = 10$ ) of the first post-rest peak current. The  $\beta_1$  subunit dramatically reduced the use-dependent properties of hH1 Na channels as it did in  $\mu 1$  Na channels. The relief of use-dependent decay by the  $\beta_1$  subunit was first evident at pulse 2 where the hH1- $\beta_1$  current equaled  $93 \pm 1\%$  ( $n = 11$ ) of the first pulse current. With continued stimulation the progressive decay of hH1- $\beta_1$  current was less pronounced, such that the pulse 20 hH1- $\beta_1$  current was  $84 \pm 1\%$  ( $n = 11$ ) of the first pulse. The significant decrease ( $p < 0.001$ ) in the amount of use-dependent decay of hH1- $\beta_1$  currents by both short- and long-duration pulse trains further supports a functional association of the  $\beta_1$  subunit with hH1 Na channels.

#### *Coexpression with the $\beta_1$ Subunit Speeds Recovery from Inactivation*

Two-pulse experiments designed to quantify the time course of repriming provided further evidence that the  $\beta_1$  subunit alters inactivation gating in  $\mu 1$  and hH1 Na channels expressed in oocytes. A standard two-pulse protocol was used to examine the recovery from inactivation at  $-100$  mV. Prepulses to  $-20$  mV (1 s) were sufficient to recruit the process of slow inactivation (Rudy, 1978). As the repriming of channels occurred rapidly at  $-100$  mV, interpulse intervals were varied from 1 ms to 2 s. In these experiments, the oocytes were held at  $-100$  mV for a long enough time (15 s for  $\mu 1$ - $\beta_1$ , 45 s for  $\mu 1$ , 15 s for hH1- $\beta_1$  and 30 s for hH1 Na channels) to allow full recovery of peak current between trials. The amount of recovery was assessed by the ratio of the second pulse current to the first pulse current (Fig. 10). Coexpression with the  $\beta_1$  subunit significantly abbreviated the time required for repriming of current ( $\mu 1$ - $\beta_1$  vs  $\mu 1$ ,  $p < 0.001$ ; hH1- $\beta_1$  vs hH1,  $p < 0.001$ ). The recovery from inactivation data were only fit adequately by third-order exponential decay functions in which all three time constants were decreased to describe the repriming of  $\alpha$ - $\beta_1$  channels compared to  $\alpha$ -only channels (see legend to Fig. 10 for fitting parameters).

#### DISCUSSION

Modification of Na channel function by the  $\beta_1$  subunit has been established for brain and skeletal muscle Na channels expressed in oocytes (Krafte, Goldin, Auld, Dunn, Davidson, and Lester, 1990; Isom et al., 1992; Cannon et al., 1993). We have performed parallel sets of experiments on  $\mu 1$  and hH1 Na channels that confirm the functional association of the  $\beta_1$  subunit with the rat skeletal muscle  $\alpha$  subunit and provide the first evidence that  $\beta_1$  subunit RNA coinjected with cardiac  $\alpha$  subunit RNA modifies the function of the oocyte-expressed Na channels.

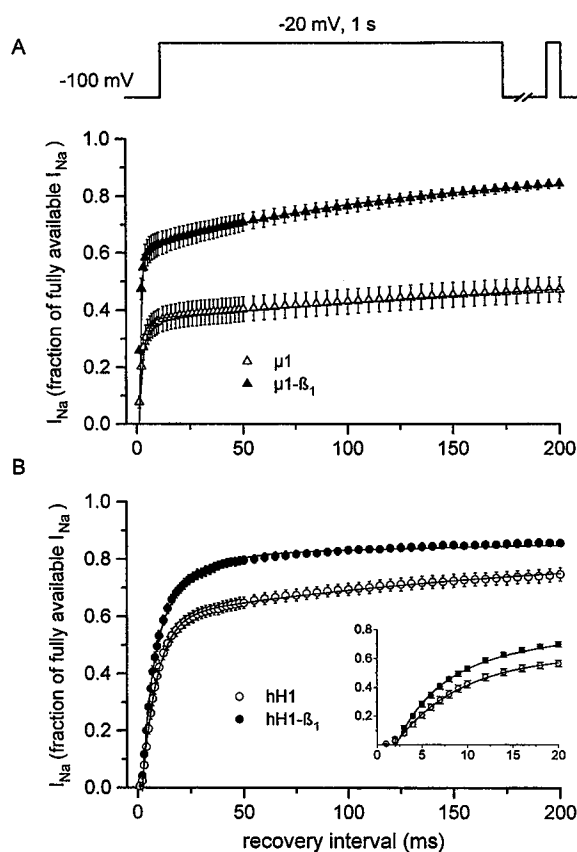


FIGURE 10. Recovery from inactivation of  $\mu 1$  vs  $\mu 1$ - $\beta_1$  (A) and hH1 vs hH1- $\beta_1$  (B) Na currents. A standard two-pulse protocol was used to compare recovery from inactivation of  $\alpha$ -only and  $\alpha$ - $\beta_1$  channels at the holding potential of  $-100$  mV as shown in the voltage pulse (*top*). Channels were inactivated ( $-20$  mV, 1 s) and recovery measured at  $-20$  mV (40 ms) after a variable recovery interval (see Results for details). The repriming data were best fit by a third order exponential decay function. The time constants were obtained by repetitive fitting sessions and then fixed while the amplitudes of each exponential were allowed to float for the final fitting. The fitting parameters for recovery of  $\mu 1$  channels are:  $t_1 = 2.1$  ms,  $A_1 = -0.36$ ,  $t_2 = 350$  ms,  $A_2 = -0.17$ ,  $t_3 = 3,000$  ms,  $A_3 = -0.47$ . Repriming of  $\mu 1$ - $\beta_1$  currents (A) was markedly hastened:  $t_1 = 1$  ms,  $A_1 = -0.60$ ,  $t_2 = 100$  ms,  $A_2 = -0.23$ ,  $t_3 = 900$  ms,  $A_3 = -0.17$ . In contrast to  $\mu 1$ ,

hH1  $\alpha$ -only channels reprime rapidly ( $t_1 = 7$  ms,  $A_1 = -0.59$ ,  $t_2 = 160$  ms,  $A_2 = -0.19$ ,  $t_3 = 1,800$  ms,  $A_3 = -0.21$ ) although after an obvious deactivation period (1–2 ms, see B, *inset* at faster time base). Similar to its effects on repriming of  $\mu 1$  channels, coinjection with  $\beta_1$  further speeds recovery from inactivation of hH1 channels (B). The fitting parameters for hH1- $\beta_1$  repriming are:  $t_1 = 4$  ms,  $A_1 = -0.45$ ,  $t_2 = 16$  ms,  $A_2 = -0.38$ ,  $t_3 = 900$  ms,  $A_3 = -0.17$ .

### Modulation of $\mu 1$ Channels by $\beta_1$ Subunit

Early reports of functional expression of cloned mammalian Na channels by injection of  $\alpha$  subunit RNA (from rat brain and skeletal muscle) into oocytes noted the anomalously slow inactivation of the macroscopic current (Trimmer et al., 1989; Noda, Ikeda, Suzuki, Takeshima, Takahashi, Kuno, and Numa, 1986). The functional properties of Na channels have been shown to be more like those of native channels when expressed by injection of unfractionated RNA (Krafte et al., 1988), by coinjection of  $\alpha$  subunits with  $\beta_1$  subunit  $\delta$ RNA (Cannon et al., 1993; Isom et al., 1992), or by transient transfection into mammalian cells such as HEK 293 cells (Ukomadu, Zhou, Sigworth, and Agnew, 1992) or CHO cells (Scheuer, Auld, Boyd, Offort, Dunn, and Catterall, 1990). The rate of current decay, the voltage depen-

dence of inactivation, and the recovery from inactivation in skeletal muscle and brain Na channels are directly modulated by the  $\beta_1$  subunit (Cannon et al., 1993; Krafte et al., 1988). We coexpressed a  $\beta_1$  subunit with  $\mu 1$  Na channels in oocytes to confirm that these channel properties were modified by the functional association of the  $\beta_1$  subunit. In our laboratory, coexpression of the rat brain  $\beta_1$  subunit with the  $\mu 1$   $\alpha$  subunit increased peak  $I_{Na}$  more than 225%, shifted the voltage dependence of inactivation by 6 mV in the hyperpolarizing direction, increased the rate of macroscopic current decay, reduced the use-dependent decrease of peak  $I_{Na}$  during repetitive short- (10 ms) and long- (1 s) duration voltage steps, and dramatically accelerated recovery from inactivation.

Both the functional properties of the macroscopic current and the underlying gating behavior of single channels are modified by coinjection (Krafte et al., 1988; Krafte et al., 1990; Zhou et al., 1991). Differences in distinct gating modes underlie the rapid inactivation of  $\mu 1$  channels in HEK 293 cells compared with  $\alpha$  subunits expressed in oocytes (Ukomadu et al., 1992). Mode 1 gating, characterized by brief openings and few reopenings, predominates in HEK 293 cells (Ukomadu et al., 1992) and in coinjected oocytes (Zhou et al., 1991), while mode 2 gating, characterized by multiple reopenings or bursting behavior, occurs more frequently in oocytes expressing the  $\alpha$  subunit alone. Since both gating modes are encoded by the  $\alpha$  subunit (Moorman, Kirsch, VanDongen, Joho, and Brown, 1990), the association of the  $\beta_1$  subunit may alter the equilibrium between modes 1 and 2 towards mode 1 behavior (Zhou et al., 1991).

#### *Expression of Cardiac Na Channels*

Expression of mammalian cardiac Na channels in oocytes has not rigorously examined the requirement of the  $\beta_1$  subunit to reproduce endogenous channel function (gating), yet the expressed channels are reported to possess the physiologic and pharmacologic properties of the native channels (Gellens et al., 1992; Chahine, Chen, Barchi, Kallen, and Horn, 1992; Satin et al., 1992; Krafte et al., 1991). Makita et al. (1994) found no evidence for a functional association between the hH1  $\alpha$  subunit and the  $\beta_1$  subunit: the human  $\beta_1$  subunit (H $\beta_{1A}$ ) cloned from heart and skeletal muscle did not alter the kinetics or the voltage dependence of inactivation of hH1 Na channels expressed in oocytes. We have examined the functional properties of hH1 Na channels expressed in oocytes with and without the  $\beta_1$  subunit to establish whether  $\beta_1$  modulates hH1 Na channel function. In line with our results in  $\mu 1$  Na channels, coexpression of rat brain  $\beta_1$  subunit with hH1 Na channels increased peak  $I_{Na}$  by 240%, accelerated the decay of macroscopic currents, and reduced use-dependent decay of  $I_{Na}$  during trains of voltage steps. Data collected from cell-attached patches confirmed that changes in the macroscopic inactivation kinetics, observed under two-electrode voltage clamp, were a genuine result of  $\beta_1$  subunit association: times to 75% decay of hH1- $\beta_1$  ensemble average currents were shorter than for hH1. We have shown that coexpression with the  $\beta_1$  subunit modifies inactivation kinetics, repriming and other functional properties of hH1 Na currents recorded in *Xenopus* oocytes. These results support a physiologically relevant functional association of  $\beta_1$  subunit with the human cardiac Na channel  $\alpha$  subunit.



### *Comparison of Primary Structure*

The primary structure of the hH1  $\alpha$  subunit sequence is most similar (>90% primary structure identity) to rat heart (RH1) and to the equivalent isoform found in denervated rat skeletal muscle (rSkM2) (Gellens et al., 1992). However, the extent of structural homology between  $\mu_1$  (rSkM1) and hH1 is much lower (59% amino acid sequence identity) (Gellens et al., 1992). The greatest homology resides within the membrane-spanning regions of hH1 and  $\mu_1$ , while the interdomain linkers I-II and II-III are divergent (<25% structural identity) (Gellens et al., 1992). Thus, it is not surprising that the electrophysiologic properties of  $\mu_1$  and hH1 Na channels differ. Nevertheless, the functional effects of  $\beta_1$  subunit coexpression are fundamentally conserved in the two isoforms, hinting that the region which associates with  $\beta_1$  will prove to be at least partially homologous.

Although this study has provided functional evidence for interactions between the rat brain  $\beta_1$  subunit and the human heart and rat skeletal muscle  $\alpha$  subunits, the structural homology amongst the  $\beta_1$  subunit isoforms is so high that similar results are anticipated with coinjection of the corresponding tissue- and species-specific  $\beta_1$  subunits. A very high degree of structural homology among brain, heart and skeletal muscle  $\beta_1$  subunits has been reported (Sutkowski and Catterall, 1990; Makita et al., 1994). Sutkowski and Catterall (1990) used antigen affinity chromatography to purify anti- $\beta_1$  subunit antibodies to rat brain  $\beta_1$  and found that these antibodies also recognized  $\beta_1$  in rat heart and skeletal muscle. Makita et al. (1994) reported that human heart and skeletal muscle  $\beta_1$  cDNA nucleotide sequences are identical and possess 96% sequence identity to rat brain  $\beta_1$  which has the identical cDNA sequence as rat heart  $\beta_1$ . In fact, the  $\beta_1$  subunit has been mapped to a single gene (Tong, Potts, Rochelle, Seldin, and Agnew, 1993; Makita et al., 1994). There is also functional evidence that all  $\beta_1$  subunits modulate Na channel properties in similar ways. Zhou et al. (1991) found that coinjection of  $\beta_1$  RNA from either skeletal muscle or brain with  $\mu_1$  RNA increased a fast component of macroscopic  $\mu_1$  current by inducing alterations in modal gating behavior. Bennett, Makita, and George (1993) obtained similar results using rat heart  $\beta_1$  to restore the normal gating behavior of the human skeletal muscle Na channel. These findings suggest that brain, heart, and skeletal muscle  $\beta_1$  subunits associate with and modulate Na channel  $\alpha$  subunit function in similar ways without demonstrating tissue specificity.

### *hH1- $\beta_1$ Channels More Closely Reproduce Endogenous Channel Function*

A comparison of results obtained in this study to the functional properties reported for native heart channels indicate that coexpressed hH1 Na channels composed of  $\alpha$  and  $\beta_1$  subunits behave like cardiac channels in vivo. In isolated cardiac myocytes or Purkinje fiber cells, the half-inactivation potentials occur at  $-80$  mV, nearly the same as hH1- $\beta_1$  in oocytes (Satin et al., 1992; Lee, Matsuda, Reynertson, Martins, and Shibata, 1993), or at more hyperpolarized potentials (Jia, Furukawa, Singer, Sakakibara, Eager, Backer, Arentzen, and Wasserstrom, 1993; Makielski, Sheets, Hanck, January, and Fozzard, 1987). The decay of whole-cell Na currents recorded in cardiac cells is extremely fast: when fit as a biexponential process, native  $I_{Na}$  decays with a fast time constant of inactivation of  $\sim 2$  ms at  $-40$  mV, which decreases

to  $<1$  ms at more positive potentials (Satin et al., 1992; Brown, Lee, and Powell, 1981; Makielski et al., 1987). Coexpressed hH1- $\beta_1$  channels produce macroscopic and ensemble average currents that more closely reproduce such rapid inactivation kinetics than do channels expressed from the hH1  $\alpha$  subunit alone. Native heart Na channels demonstrate no use-dependent decay of peak current even at stimulation rates of 1–4 Hz (Bean, Cohen, and Tsien, 1983; Lee et al., 1993; Jia et al., 1993). Although repetitive pulsing (0.5 Hz) in oocytes produced only a small decrement of hH1 current, hH1- $\beta_1$  currents were even more resistant to such use-dependent effects. At hyperpolarized potentials, recovery from inactivation in native heart Na channels can be described by two exponential terms, with the larger portion of recovery occurring with a fast time constant of 3–6 ms (Jia et al., 1993; Brown et al., 1981). Recovery from inactivation by hH1- $\beta_1$  channels is similar to that in native channels: the amplitude of the fast component is largest, with a time constant equal to 4 ms (Fig. 10 B) compared to 7 ms for hH1 channels. Thus, many important features of endogenous cardiac Na channel gating, including rapid macroscopic current decay, the virtual absence of use-dependent decay of the peak current, and rapid recovery from inactivation, are more closely reproduced by hH1  $\alpha$ - $\beta_1$  than hH1  $\alpha$ -only Na channels.

#### *Coexpression of $\beta_1$ Affects Gating but Not Permeation*

Permeation in  $\mu_1$  and hH1 channels is not altered by coexpression with the  $\beta_1$  subunit: there were no significant differences in the unitary current amplitudes or the slope conductances of the coexpressed channels vs those encoded by  $\alpha$  only. The whole-cell experiments reveal that the primary effect of the  $\beta_1$  subunit association with hH1 and  $\mu_1$  channels involves inactivation gating:  $\beta_1$  speeds macroscopic current inactivation and increases the rate of recovery from inactivation. The apparent explanation for the enhancement of macroscopic inactivation is that  $\beta_1$  modifies entry into and return from the inactivated state. Within the limitations of the data collected from cell-attached patches in this study (no one-channel patches), hH1- $\beta_1$  channels had shorter mean open times ( $0.89 \pm 0.07$  ms at  $-40$  mV,  $n = 6$ ) compared to hH1 channels ( $1.10 \pm 0.10$  ms,  $n = 6$ ), and fewer reopenings. Both of these changes in single-channel gating would tend to hasten macroscopic current decay.

Given the lack of changes in permeation, there are two potential mechanisms by which coexpression with the  $\beta_1$  subunit increases hH1 macroscopic current density: an increase in the number of functional channels, and/or an increase in the unitary open probability. We were able to estimate the maximal open probability of hH1 and hH1- $\beta_1$  channels from the single-channel data obtained in this study. The single-channel probability of opening is  $P_o = I/Ni$  where  $I$  is the size of the peak ensemble average current,  $N$  is the number of active channels contained in the patch, and  $i$  is the unitary current amplitude. Measurements of  $P_o$  at two different potentials ( $-40$  mV,  $-20$  mV) indicate that coexpression with the  $\beta_1$  subunit does not significantly increase hH1 channel open probability. At  $-40$  mV,  $P_o$  equaled  $0.22 \pm 0.05$  in hH1- $\beta_1$  channels ( $n = 4$ ) and  $0.21 \pm 0.04$  in hH1 channels ( $n = 5$ ). While  $P_o$  tended to increase at  $-20$  mV in hH1- $\beta_1$  channels ( $0.36 \pm 0.08$ ,  $n = 4$ ) compared to hH1 channels ( $0.26 \pm 0.06$ ,  $n = 3$ ), the effect did not reach statistical signifi-

cance by one-way ANOVA. Even if genuine, these modest increases in open probability do not come close to accounting for the 2.4-fold increase in macroscopic current in hH1- $\beta_1$  oocytes relative to those expressing the  $\alpha$  subunit alone. Thus, the predominant effect is an increase in the number of functional channels.

It is instructive to compare the mechanism of the increased expression of hH1 Na current by  $\beta_1$  subunit interactions to analogous results in Ca channels. Neely, Wei, Olcese, Birnbaumer, and Stefani (1993) reported that coexpression of the  $\beta$  subunit with the  $\alpha_{1C}$  subunit does not increase the expression of Ca channels: measurements of gating currents and estimates of channel densities were not significantly different between coinjected oocytes and oocytes injected with the  $\alpha_{1C}$  subunit alone. A different picture emerges from studies in mammalian HEK293 cells, where coexpression of  $\alpha_{1C}$  and  $\beta$  increases the densities of Ca current and dihydropyridine receptors (Pérez-García, Kamp, and Marbán, 1995) while augmenting the gating currents (Kamp, Pérez-García, and Marbán, 1995). The latter results closely parallel those reported here, suggesting that  $\alpha$  subunits may generally facilitate the packaging and assembly of functional ion channels.

This work was supported by grants from the National Institutes of Health (RO1 HL52768 to E. Marbán and KO8 HL02421 to G. F. Tomaselli), the Canadian Heart and Stroke Foundation and MRC, Canada (to N. Chiamvimonvat), the Fundación Ramon y Areces (to M. T. Pérez-García), and the American Heart Association Maryland Affiliate (postdoctoral fellowship to H. B. Nuss).

*Original version received 3 August 1994 and accepted version received 13 June 1995.*

#### REFERENCES

- Auld, V. J., A. L. Goldin, D. S. Krafte, J. Marshall, J. M. Dunn, W. A. Catterall, H. A. Lester, N. Davidson, and R. J. Dunn. 1988. A rat brain Na<sup>+</sup> channel  $\alpha$  subunit with novel gating properties. *Neuron*. 1:449–461.
- Bean, B. P., C. J. Cohen, and R. W. Tsien. 1983. Lidocaine block of cardiac sodium channels. *The Journal of General Physiology*. 81:613–642.
- Bennett, P. B. Jr., N. Makita, and A. L. George, Jr. 1993. A molecular basis for gating mode transitions in human skeletal muscle Na<sup>+</sup> channels. *FEBS Letters*. 326:21–24.
- Brown, A. M., K. S. Lee, and T. Powell. 1981. Sodium current in single rat heart muscle cells. *Journal of Physiology*. 318:479–500.
- Cannon, S. C., A. I. McClatchey, and J. F. Gusella. 1993. Modification of the Na<sup>+</sup> current conducted by the rat skeletal muscle  $\alpha$  subunit by coexpression with a human brain  $\alpha$  subunit. *Pflügers Archiv*. 423:155–157.
- Catterall, W. A. 1994. Cellular and molecular biology of voltage-gated sodium channels. *Physiological Reviews*. 72:S15–S48.
- Chahine, M., L. Q. Chen, R. L. Barchi, R. G. Kallen, and R. Horn. 1992. Lidocaine block of human heart sodium channels expressed in *Xenopus* oocytes. *Journal of Molecular and Cellular Cardiology*. 24:1231–1236.
- Cole, K. S. 1972. Membranes, ions and impulses: a chapter of classical biophysics. University of California Press, Berkeley, CA. 325–337.
- Colquhoun, D., and F. S. Sigworth. 1983. Fitting and statistical analysis of single-channel records. In *Single-Channel Recording*. B. Sakmann and E. Neher, editors. Plenum Publishing Corp., NY. 191–263.
- Gellens, M. E., A. L. George, L. Chen, M. Chahine, R. Horn, R. L. Barchi, and R. G. Kallen. 1992. Pri-

- mary structure and functional expression of the human cardiac tetrodotoxin-insensitive voltage-dependent sodium channel. *Proceedings of the National Academy of Sciences, USA*. 89:554–558.
- Goldin, A. L., T. Snutch, H. Lubbert, A. Dowsett, J. Marshall, V. Auld, W. Downey, L. C. Fritz, H. A. Lester, R. Dunn, W. A. Catterall, and N. Davidson. 1986. Messenger RNA coding for only the  $\alpha$  subunit of the rat brain Na channel is sufficient for expression of functional channels in *Xenopus* oocytes. *Proceedings of the National Academy of Sciences, USA*. 83:7503–7507.
- Hille, B. 1992. Ionic channels of excitable membranes. Second edition. Sinauer Associates Inc., Sunderland, MA.
- Isom, L. L., K. S. DeJongh, D. E. Patton, B. F. X. Reber, J. Offord, H. Charbonneau, K. Walsh, A. L. Goldin, and W. A. Catterall. 1992. Primary structure and functional expression of the  $\alpha_1$  subunit of the rat brain sodium channel. *Science*. 256:839–842.
- Isom, L. L., K. S. DeJongh, and W. A. Catterall. 1994. Auxiliary subunits of voltage-gated ion channels. *Neuron*. 12:1183–1194.
- Jia, H., T. Furukawa, D. H. Singer, Y. Sakakibara, S. Eager, C. Backer, C. Arentzen, and J. A. Wasserstrom. 1993. Characteristics of lidocaine block of sodium channels in single human atrial cells. *The Journal of Pharmacology and Experimental Therapeutics*. 264:1275–1284.
- Kamp, T. J., M. T. Pérez-García, and E. Marbán. 1995. Coexpression of  $\alpha$  subunit with L-type calcium channel  $\alpha_{1C}$  subunit in HEK293 cells increases ionic and gating currents. *Biophysical Journal*. 68:A349. (Abstr.)
- Krafte, D. S., T. P. Snutch, J. P. Leonard, N. Davidson, and H. A. Lester. 1988. Evidence for the involvement of more than one mRNA species in controlling the inactivation process of rat and rabbit brain Na channels expressed in *Xenopus* oocytes. *The Journal of Neuroscience*. 8:2859–2868.
- Krafte, D. S., A. L. Goldin, V. J. Auld, R. J. Dunn, N. Davidson, and H. A. Lester. 1990. Inactivation of cloned Na channels expressed in *Xenopus* oocytes. *The Journal of General Physiology*. 96:689–706.
- Krafte, D. S., W. A. Volberg, K. Dillon, and A. M. Ezrin. 1991. Expression of cardiac Na channels with appropriate physiological and pharmacological properties in *Xenopus* oocytes. *Proceedings of the National Academy of Sciences, USA*. 88:4071–4074.
- Krieg, P. A., and D. A. Melton. 1984. Functional messenger RNAs are produced by SP6 in vitro transcription of cloned cDNAs. *Nucleic Acids Research*. 12:7057–7070.
- Lee, H. C., J. J. Matsuda, S. L. Reynertson, J. B. Martins, and E. F. Shibata. 1993. Reversal of lidocaine effects on sodium currents by isoproterenol in rabbit hearts and heart cells. *Journal of Clinical Investigation*. 91:693–701.
- Makielski, J. C., M. F. Sheets, D. A. Hanck, C. T. January, and H. A. Fozzard. 1987. Sodium current in voltage clamped internally perfused canine cardiac Purkinje cells. *Biophysical Journal*. 52:1–11.
- Makita, N., P. B. Bennett, and A. L. George, Jr. 1994. Voltage-gated Na<sup>+</sup> channel  $\beta_1$  subunit mRNA expressed in adult human skeletal muscle, heart, and brain is encoded by a single gene. *The Journal of Biological Chemistry*. 269:7571–7578.
- Methfessel, C., V. Witzemann, T. Takahashi, M. Mishina, S. Numa, and B. Sakmann. 1986. Patch clamp measurements on *Xenopus laevis* oocytes: currents through endogenous channels and implanted acetylcholine receptor and sodium channels. *Pflügers Archiv*. 407:577–588.
- Moorman, J. R., G. E. Kirsch, A. M. J. VanDongen, R. H. Joho, and A. M. Brown. 1990. Fast and slow gating of sodium channels encoded by a single mRNA. *Neuron*. 4:243–252.
- Neely, A., X. Wei, R. Olcese, L. Birnbaumer, and E. Stefani. 1993. Potentiation by the  $\alpha$  subunit of the ratio of the ionic current to the charge movement in the cardiac calcium channel. *Science*. 262:575–578.
- Noda, M., T. Ikeda, H. Suzuki, H. Takeshima, T. Takahashi, M. Kuno, and S. Numa. 1986. Expression of functional sodium channels from cloned cDNA. *Nature*. 322:826–828.
- Pérez-García, M. T., T. J. Kamp, and E. Marbán. 1995. Functional properties of cardiac L-type cal-

- cium channels transiently expressed in HEK293 cells. *The Journal of General Physiology*. 105:1–18.
- Rudy, B. 1978. Slow inactivation of the sodium conductance in squid giant axons. Pronase resistance. *Journal of Physiology*. 283:1–21.
- Satin, J., J. W. Kyle, M. Chen, R. B. Rogart, and H. A. Fozzard. 1992. The cloned cardiac Na channel  $\alpha$ -subunit expressed in *Xenopus* oocytes show gating and blocking properties of native channels. *The Journal of Membrane Biology*. 130:11–22.
- Scheuer, T., V. J. Auld, S. Boyd, J. Offort, R. Dunn, and W. A. Catterall. 1990. Functional properties of rat brain sodium channels expressed in a somatic cell line. *Science*. 247:854–858.
- Sutkowski, E. M., and W. A. Catterall. 1990.  $\alpha_1$  subunits of sodium channels. *The Journal of Biological Chemistry*. 265:12393–12399.
- Tong, J., J. F. Potts, J. M. Rochelle, M. F. Seldin, and W. S. Agnew. 1993. A single  $\beta_1$  subunit mapped to mouse chromosome 7 may be a common component of Na channel isoforms from brain, skeletal muscle and heart. *Biochemical and Biophysical Research Communications*. 195:679–685.
- Trimmer, J. S., S. S. Cooperman, S. A. Tomiko, J. Zhou, S. M. Crean, M. B. Boyle, R. G. Kallen, S. A. Sheng, R. L. Barchi, F. J. Sigworth, R. H. Goodman, W. S. Agnew, and G. Mandel. 1989. Primary structure and functional expression of a mammalian skeletal muscle sodium channel. *Neuron*. 3: 33–49.
- Ukomadu, C., J. Zhou, F. J. Sigworth, and W. S. Agnew. 1992.  $\mu 1$  Na<sup>+</sup> channels expressed transiently in human embryonic kidney cells: biochemical and biophysical properties. *Neuron*. 8:663–676.
- Wallner, M., L. Weigl, P. Meera, and I. Lotan. 1993. Modulation of the skeletal muscle sodium channel alpha-subunit by the beta 1-subunit. *FEBS Letters*. 336:535–539.
- Zhou, J., J. F. Potts, J. S. Trimmer, W. S. Agnew, and F. J. Sigworth. 1991. Multiple gating modes and the effect of modulating factors on the  $\mu 1$  sodium channel. *Neuron*. 7:775–785.